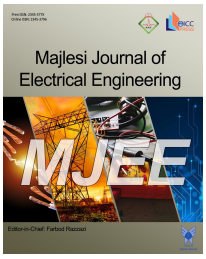

Majlesi J. Electr. Eng. 2026; 20(1) : 96-112

Majlesi Journal of Electrical Engineering (MJEE)

https://dx.doi.org/10.57647/mjee.2026.2001.07

Original Research

Efficiency Improvement of MEMS-based Solar Cells by Optimizing the Structure and Dimensions of Piezoelectric-based Vertical Nanowires

Amir Saljooghi, Hadi Saghafi*, Mohammad Rouhollah Yazdani, Mohammadali Abbasian

Department of Electrical Engineering, Isf.C., Islamic Azad University, Isfahan, Iran

***Corresponding author:** h.saghafi@iau.ac.ir

Article History

Received:
15 June 2025

Revised:
21 September 2025

Accepted:
15 December 2025

Published in Issue:
31 March 2026

Abstract:

The global energy crisis and environmental challenges have drawn increasing attention from researchers toward the development of renewable energy technologies, particularly solar energy. Among the emerging technologies in this field, Micro-Electro-Mechanical Systems (MEMS) have gained considerable interest in recent years due to the relatively low efficiency of conventional photovoltaic modules. MEMS-based technologies offer a wide range of applications, including light control, thermal management, and enhancement of optical properties. Another technology that has recently attracted attention in solar energy research is piezoelectric technology. The integration of piezoelectric materials enables the generation of electrical energy from mechanical stresses induced by temperature differences across distinct surfaces, thereby enhancing the energy output and overall efficiency of solar cells. This article describes the structure of a hybrid solar cell based on MEMS technology, the use of vertical nanowires, and the piezoelectric properties of materials. It can be reached to higher efficiency by choosing suitable materials and changing some structural parameters. The proposed structure consists of a two-layer triangular cantilever (aluminum and silicon oxide). The piezoelectric layer is made arranging a different structure of nanowires and increasing the area covered by nanowires. Despite previous works present only one structure, this paper tries to present and compare different structures for more flexible structure selection. The simulation results using COMSOL software, show improved performance compared to similar researches. Based on the results, using the proposed structure, a variable voltage with a maximum value of 1.15 volts and the best efficiency of 46.11% (in a special structure) is obtained.

Keywords: Solar cells; Micro-Electro-Mechanical Systems (MEMS); Piezoelectric effect; Vertical nanowire

Cite this article: Saljooghi A, Saghafi H, Yazdani MR, Abbasian M. Efficiency Improvement of MEMS-based Solar Cells by Optimizing the Structure and Dimensions of Piezoelectric-based Vertical Nanowires. Majlesi J. Electr. Eng. 2026;20(1): 96-112. https://doi.org/10.57647/j.ijnd.2026.1702.01

1. Introduction

Micro-Electro-Mechanical Systems (MEMS), micro technologies or microelectromechanical systems, are a combination of mechanical components, mechanical arms, sensors electronic components. These very small micrometer structures are based on electronic chip technology. The first structures of MEMS were simple accelerometers and temperature and pressure sensors. MEMS technology has significant advantages such as scalability, high measurement sensitivity, improved high-frequency performance, low energy consumption, small dimensions, and the possibility of integration in small systems light, have low power consumption and short start-up times [1]. It also offers the possibility of improving efficiency in applications such as solar cells, while the main disadvantage is the high cost in the manufacturing and commissioning phase [2]. Experiences gained from recent applications of MEMS have enabled this technology to operate in new fields such as

BioMEMS, wireless information transmission, including optical communication systems [4].

With respect to the large spectrum of applications, MEMS enjoy a rich variety [5]. RF MEMS switches commonly use mechanical movement to exhibit a short circuit or open circuit in the RF transmission line Or MEMS acoustic sensor [6].

So far, various structures have been introduced and used as solar cells [7, 8]. Therefore, MEMS technology has also considered the construction of solar cells to use solar energy [9]. This technology tries to use as much of the energy received by the sun as possible by using different methods [10, 11]. So far, different structures have been proposed as high-efficiency solar cells. The different types of common solar cells that have been introduced to generate electricity can be classified into different groups based on their functional mechanism the same as Perovskite-Silicon solar cell [12]. One of these structures is a solar cell based on MEMS technology. MEMS technology has started to introduce structures called MEMS solar cells with the aim of providing a simpler, smaller structure with lower manufacturing costs and, what is essential in this regard, more energy extraction from solar energy. The MEMS solar cells presented so far do not have the same functional mechanism; so how each cell works is different [13].

Some materials and crystals can convert mechanical energy into electrical and vice versa, this ability is called piezoelectric effect, which maybe in direct or inverse direction. Due to the direct piezoelectric effect, stretching and bending in the material creates an electric charge on the surface of the crystal cell and establishes an electrical potential difference [14]. The reverse piezoelectric effect, the application of an electric field to a piezoelectric crystal causes mechanical vibrations in its structure. The piezoelectric interpretive equations are defined as:

$$D_i = \varepsilon_{ij}^T + d_{ij}T_j \tag{1}$$

$$S_i = d_{ij}E_j + S_{ij}^E T_j \tag{2}$$

where D and E are the electric displacement and electric field, respectively, ε is the dielectric permittivity of the material and S the elastic function of the material. The superscripts T and E indicate that the values of the coefficients in the constant voltage and electric field are calculated, respectively. The d_{ij} constant in the above equations represents the piezoelectric charge/strain constant [15].

Reference [16] uses MEMS technology to convert solar radiation into solar energy. Conventional solar cells, on the other hand, use solid-state PN junctions. In this work, it uses a Nano-scale vacuum gap, or Nano-gap, to generate an electric charge in response to solar radiation which prevents the electron from recombining with the hole and reduces electron loss and thus increases efficiency. Reference [17] presents a solar energy picker that is a reliable solution for designing self-powered microsystems. This invention intended to have high operating frequency, small size, and controllable capacitive properties. This unit combines conventional energy harvesting with RF MEMS to achieve adjustable output power and scalability. This structure consists of an RF MEMS switch and a photoactive layer responsible for generating the load.

The Details of a new design of a MEMS-based solar cell are presented in Fig. 1 [3]. Based on Fig. 1, the main parts of the structure are:

(1) Bilayer Micro Cantilever (Semiconductor-metal),

(2) Piezoelectric thin layer attached to BMC,

(3) Movable panel with apertures,

(4) Fixed panel with apertures,

(5) Two charged electrodes, one connected to the BMC and the other connected to the moving panel,

(6) Focusing lenses collect the most power from incoming sunlight [3].

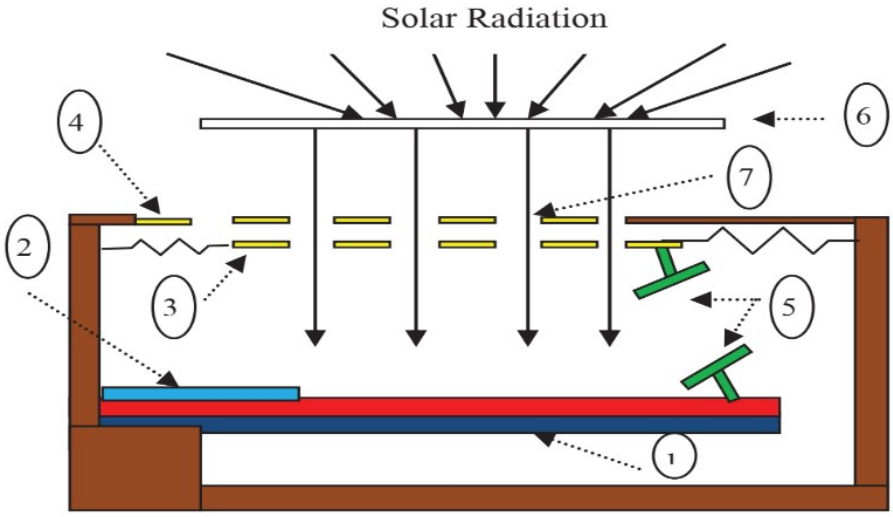

Figure 1. Solar cell structure presented in [3].

https://dx.doi.org/10.57647/mjee.2026.2001.07

This structure works in such a way that when the BMC is exposed to sunlight, it absorbs some of the incoming solar energy. Part of the energy absorbed in the layers is converted to heat, which leads to heat stress in each of the two metal and semiconductor layers. Since the two layers have different coefficients of thermal expansion, the amount of stress created will be different. The other part of the absorbed energy produces free charge carriers in the semiconductor layer, which causes electronic stress. Due to the difference in surface stress in each bilayer, the BMC will deviate to a certain extent, which depends on the input power and dimensions of the BMC.

During BMC deflection, the moving plate shifts between the two electrodes due to repulsive force. This displacement as shown in Fig. 2, causes a mismatch between the apertures of the moving panel and the fixed panel. As a result, the amount of solar power reaching the BMC level is reduced. When BMC returns to its original position, the moving panel returns to its original position. The input power to the BMC level then increases again, causing it to deviate. This process will constantly be repeated. The BMC response to changes in input power is a mechanical oscillation that is easily converted to electrical energy by a thin piezoelectric layer. In the proposed design, ALN nanowire for high efficiency are placed in the solar cell to increase the piezoelectric effect efficiency. The simulation results for the proposed design, which has an area of about 0.004 mm^2, show an efficiency of 46.11% and an open circuit voltage of 1.15 V. The main novelties of the presented work are enumerated, as follows:

- In the proposed plan of this research, which is a combination of MEMS solar cells and piezoelectric devices in series, the anode of the solar cell is connected to the piezoelectric cathode, and the output electrodes of the assembly are considered as the cathode of the solar cell and the piezoelectric anode.
- Placement of a large number of nanowires with tiny space.
- In the proposed design of this research, the piezoelectric length is up to 60 µm and higher efficiency, provided that the upper part of the piezoelectric device is also considered fixed like the fixed end of the beam.
- To increase the tension. In the piezoelectric part, the proposed structure is implemented in a triangular shape so that its tension value is minimized in the place (the free end of the beam) where the voltage is not needed.

This paper is divided to four sections, in the second section the proposed solar cell design is introduced and the third section is dedicated to the simulation results of the proposed improved design. Finally, in the fourth section, a general comparison of the results of the proposed design with several similar tasks is presented and discussed.

2. The proposed design

This study aims to increase the efficiency of solar cells with new technologies (MEMS) since it is not possible to achieve the level of efficiency of MEMS solar cells with a conventional solar cell alone. For this reason, the proposed design of this study is a combination of conventional and piezoelectric solar cells (hybrid solar cells). Nanowires acquire unique electronic and optical

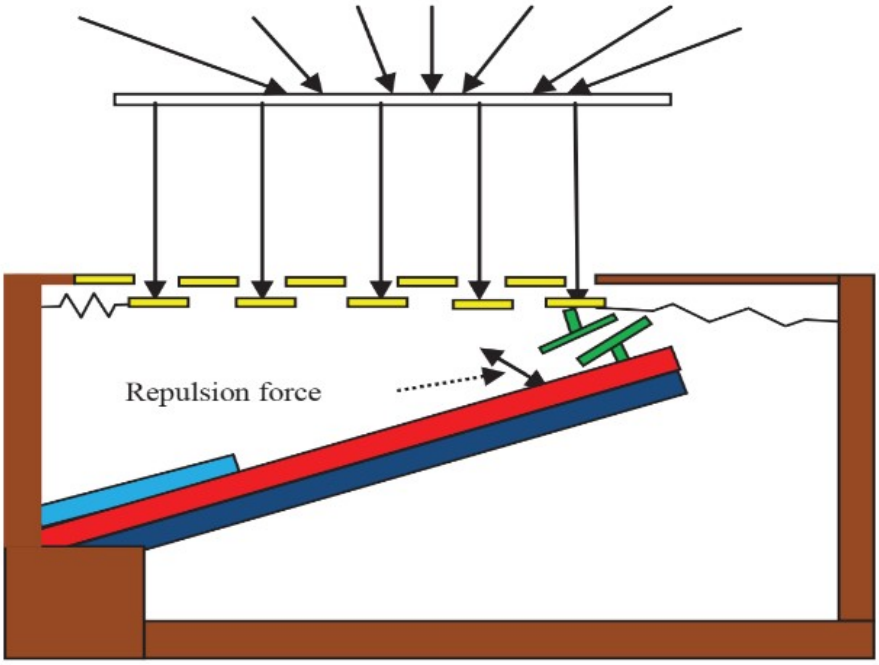

Figure 2. The solar cell proposed in [3] during deflection

https://dx.doi.org/10.57647/mjee.2026.2001.07

properties. Because of the significant potential energy conversion efficiency and optical advantages, nanowires are beneficial for the fabrication of photovoltaic (PV) devices.

The proposed structure in this paper, based on piezoelectric nanowires, is designed to remove the piezoelectric layer used in [18] and instead use several vertical nanowires to conduct electrical current better. Also, to increase the stress in the part related to piezoelectric nanowires, the end part of the beam is selected as a triangle to create less stress in the end part and the majority of stress is transferred to the fixed part. Therefore, the proposed design can be seen in Figs. 3 and 4. In these figures, the two structures are shown as triangular and rectangular, the part that is kept fixed in them is specified.

The proposed solar cell, based on piezoelectric nanowires, consists of a number of nanowires stacked vertically between very thin piezoelectric layers. By doing this, each nanowire acts as an electron transfer channel, and the generated electron is created by the temperature difference between the two sides of the desired piece, which is actually due to the change in the density of the penetrating carriers of electrical materials created by heat radiation. It should be noted that due to the presence of nanowires vertically, increasing the temperature and creating stress and bending in the lower cantilevers, to create a sinusoidal voltage, A sinusoidal heat flux of 1000 W/m^2 with a frequency of 80 Hz is applied [16, 18, 19]. It should also be noted that because the end of the beam and the end of the part based on nanowire and piezoelectric is kept fixed, the cooling and heating time of nanowires to pass current will be different. And in fact, it is not possible to extract the net sine voltage from this structure, but due to the presence of nanowires, the current flowing in this part is somehow directed and there are no losses due to the current flowing out of the direct path and the efficiency easily increases.

The next step after determining the structure is to determine the constituents of the proposed cell, which according to the nature of the structures based on the cantilever and according to [20], the materials that have the highest difference in coefficient of thermal expansion are used. For this reason, in this research, two materials, aluminum (Al) and copper (Cu), are used for the upper layer, and silicon dioxide (SiO_2) for the lower layer. By changing the temperature of the proposed cell and since one side of the beam is free, the difference in the coefficient of thermal expansion of the materials used causes the deformation of the cell. This deformation, which is the up-and-down of the free end of the cantilever, causes stress in the structure. One effective method to convert mechanical stress into electrical energy is by employing piezoelectric structures [21]. In this study, the piezoelectric structure is modeled as nanotubes arranged perpendicularly to the cantilever, positioned between two thin piezoelectric layers, the stress created generates a field, and due to that, the current flows between the piezoelectric layer. More information is provided in [20].

To achieve better control of the current and maximize the output, nanotubes are placed instead of a continuous piezoelectric panel. Since the current moves in different directions on a panel, the required maximum gain cannot be reached, and by placing tubes, the flow direction can be controlled and the maximum current can be received from the cell.

Of course, it should be noted that to achieve this goal it is necessary to form the most stress in the piezoelectric section, and therefore, the triangular structure is used. The triangular structure has less stress at the end due

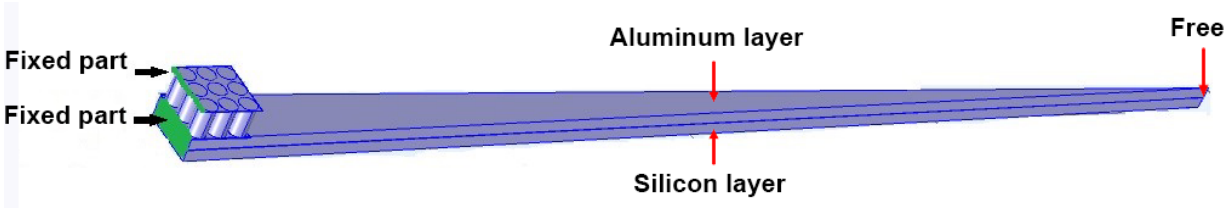

Figure 3. The proposed solar cell structure: triangular structure.

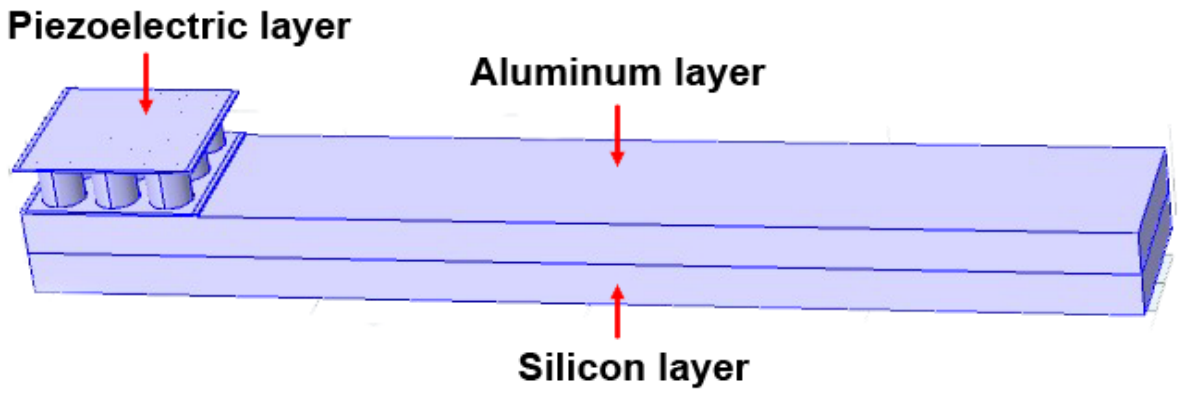

Figure 4. The proposed solar cell structure: rectangular structure.

https://dx.doi.org/10.57647/mjee.2026.2001.07

to the reduction of the surface at the free end of the cantilever and creates more stress at the fixed part of the cantilever than the rectangular cantilever. In the proposed structure for receiving electricity, the heat flux or heat entering the cell is considered sinusoidally in the simulations. However, at times, it may not be possible to apply these inputs to the structure, when the cell does not receive any temperature and cools completely. In this case, Newton's law of cooling is applied to calculate the temperature reduction and layer displacement, as shown in (3) [22].

$$\frac{dT}{dt} = K(T - T_s) \tag{3}$$

With the input flux being sinusoidal, the cell continues to heat and cool, generating voltage in the nanowire-based piezoelectric structure. By applying heat to the two-layer cantilever and increasing its temperature, as described earlier, different stresses are created in the cantilever layers, and the cantilever deflects towards the layer with a lower coefficient of thermal expansion. In order to calculate the displacement of the free end of the cantilever, a structure as illustrated in Fig. 5 is considered. In this figure, L is the length of the cantilever, b_1 and b_2 are the widths of the layers, and t_1 and t_2 are the thicknesses of the first and second layers, respectively.

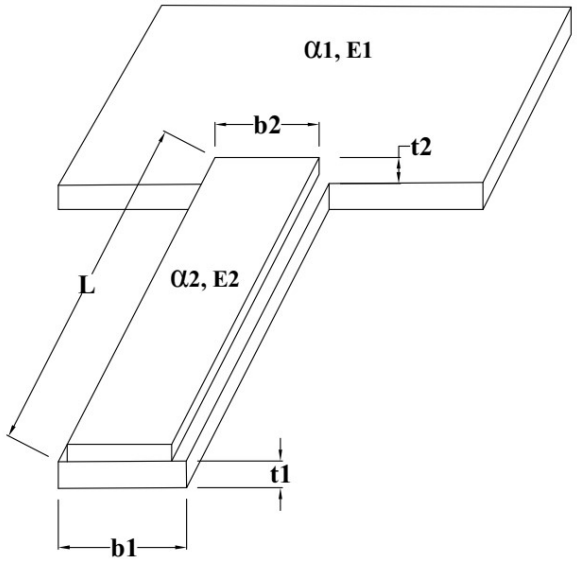

Figure 5. View of a two-layer cantilever with different materials and dimensions for each layer [23, 24].

It is assumed that the temperature distribution is uniform along the length of the cantilever. Fig. 6 shows the cross-section of a part of the proposed cell in the case of temperature rise.

P_1 represents the result of internal forces, M_1 represents the torque created in the first layer, P_2 represents the result of internal forces and M_2 the torque created in the second layer. Because the layers are paired with each other, the internal forces at each cross section must be equal:

$$P_1 = P_2 \tag{4}$$

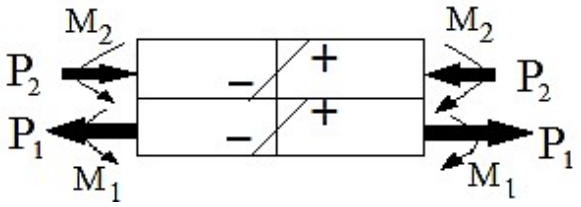

Figure 6. Forces and torques in a cross section of a two-layer cantilever [23].

which P can be calculated using the following equation:

$$\frac{P(t_1 + t_2)}{2} = M_1 + M_2 \tag{5}$$

According to the theory of beams, the equation; torque-related equation is [23].

$$M = \frac{EI}{r} \tag{6}$$

In (6), r is the radius of curvature of the beam, E is the Young's modulusof the material and I is the moment of inertia.

Finally, by arranging the equation if the width of the layers is considered equal to the radius and the amount of displacement of the free end of the cantilever, it is calculated for the change in temperature ΔT according to equations (7) [24].

$$\delta = \frac{L^2}{2r} \frac{3(\alpha_1 - \alpha_2)\Delta T L^2 (t_1 + t_2)}{t_2^2 \left[4 + 6(\frac{t_1}{t_2}) + 4(\frac{t_1}{t_2})^2 + \frac{E_1}{E_2}(\frac{t_1}{t_2})^3 + \frac{E_2}{E_1}(\frac{t_2}{t_1})\right]} \tag{7}$$

Another factor is the slope of the free end of the two-layer cantilever, which must be taken into account. Considering the usual assumptions of simple beam theory and applying the equilibrium and equations governing the system, the internal forces and bending moments are calculated [24] for example:

$$M_1 = \frac{E_1 t_1^2 (\Delta\alpha)(\Delta T)}{2\left[\frac{3\lambda\zeta(1+\zeta^2)+(1+\lambda\zeta)(1+\lambda\zeta^3)}{\lambda\zeta^2(1+\zeta)}\right]} \tag{8}$$

$$\theta = \frac{6(\Delta\alpha)(\Delta T)L}{t_1\left[\frac{3\lambda\zeta(1+\zeta)^2+(1+\lambda\zeta)(1+\lambda\zeta^3)}{\lambda\zeta(1+\zeta)^2}\right]} \tag{9}$$

In the above equations
$\lambda = E_1/E_2$ is the Young's modulus ratio.
$\zeta = t_1/t_2$ is the thickness ratio.
$\Delta\alpha$ is the difference between the coefficients of thermal expansion of the material.

When the bilayer cantilever is subjected to a uniform temperature difference, the free end deviates, and a slope is created in the structure. The temperature difference is relative to the ambient temperature. This slope is obtained as
From (9), it is shown that The free end slope of a bilayer thermal cantilever depends only on the materials used

https://dx.doi.org/10.57647/mjee.2026.2001.07

(values of E and α) and the thickness ratio for a given temperature difference. Therefore, θ optimization is more effective concerning the thickness ratio for a given material pair. This implies that for a given $\Delta\alpha$ and a constant dimension ratio ($\beta = L/t$) under a constant temperature difference ΔT, the denominator of (9) is minimized to achieve maximum efficiency. The deflection slope is optimized because the higher the beam deflection, the greater the tensile stress in the piezoelectric layer. To optimize normalized slope (θ_n) is defined as follows:

$$\theta_n = \frac{\theta}{6(\Delta T)\beta} = \frac{\Delta\alpha}{3 + Z_\theta} \tag{10}$$

$$\beta = \frac{L}{t} \tag{11}$$

$$Z_\theta = \frac{(1 + \lambda\zeta)(1 + \lambda\zeta^3)}{\lambda\zeta(1 + \zeta)^2} \tag{12}$$

In order to maximize θ for a given $\Delta\alpha$, the denominator of (12) must be fixed for $\lambda > 0$, and $\zeta > 0$ should be minimized. The optimal thickness ratio is obtained derivation equal to (13).

$$\zeta_{opt} = \frac{1}{\sqrt{\lambda}} \tag{13}$$

By optimizing (13), The primary factor affecting the free end slope is the material properties of the layers selected. Therefore, by selecting the appropriate materials, the slope of the free end and the stress in the piezoelectric layer can be greatly increased [25]. As mentioned before, two substances Al and Cu are used for the upper layer and a single material SiO_2 is used for the lower layer. In this way, the results of Al and Cu are compared to determine the effect of the difference in thermal expansion coefficient on cell efficiency. The coefficients of thermal expansion of the material according to the [26] for Al, Cu and SiO_2 are equal to 23.1, 16.4 and 0.5×10^{-6} (1/K), respectively.

3. Implementations and simulation results

In this paper, eight different designs of MEMS solar cells are presented and the results are compared with [18] and [27]. The proposed solar cell in [18] is as shown in Fig. 4, and a piezoelectric layer is used instead of the nanowires. However, in [27], a piezoelectric layer is implemented as nanowires, as shown in Fig. 4 in which the distance between the nanowires is less than 0.1 nm, and the solar cell of this reference is defined as NEMS. The close distance between the nanowires creates a field and jamming currents between the rods, and as a result, when the number of nanowires increases, the output current deviates from a sinusoidal waveform, and the cell efficiency decreases. Thus, the area of the piezoelectric section cannot be enlarged to solve this problem the nanowires in Fig. 4 are placed with larger dimensions and longer distances, which reduces the current and noise fields, and the solar cell in question is out of NEMS mode and designed as MEMS cell. The piezoelectric area can also be increased finally, to increase the stress and thus improve the efficiency of the MEMS solar cell, the structural shape of the cell has been changed from a rectangular to a triangular shape.

In fact, the disadvantages of previous structures can be summarized in the following four sections:
a) Excessive proximity of nanowires: According to [27], the number of nanowires is high, and the distance between them is inevitably small. This causes jamming currents and different fields between the nanowires and affects the output current. Placing many nanowires at a very short distance (NEMS) is a kind of approach to the reference [18], and the piezoelectric device becomes a single layer.
b) Smaller area of the piezo device: Due to large currents and noise fields caused by the very short spacing of the nanowires, the area of the piezoelectric device cannot be enlarged. The parasitic currents and electric field interactions reduce the output current and the efficiency of the proposed cell, as reported in [18].

The best piezoelectric length of 5 µm is obtained However, in the proposed design of this research, the piezoelectric length up to 60 µm has also provided a favorable answer because by increasing the number of nanowires, higher current can be obtained (with less parasitic currents due to increasing distance between nanowires) and more efficiency can be achieved. According to Fig. 7, the upper part of the piezoelectric device should be considered as fixed as the fixed end of the beams.

In Fig. 7, the upper part of the piezoelectric is also fixed, which results in a smoother voltage output. However, due to the increase in piezoelectric length (with fixed beam length), the amount of stress in this section is decreased, and the efficiency is reduced but a more sinusoidal and smoother output is obtained.
c) Low stress and consequently low efficiency: In the proposed designs so far, the proposed structure of solar cells is rectangular and easy to implement. In the proposed plan to increase the stress in the piezoelectric section, the proposed design is implemented in a triangle to minimize the value where the stress is not required.
d) Lack of presentation of results extensively: Another disadvantage of the presented articles especially [18] and [27] is the lack of results of the proposed design with different dimensions and materials. In the proposed design, eight designs are simulated separately, and the results have the necessary scope to prove the ability of the proposed design.

In this paper, the simulations were performed using COMSOL Multiphysics 5.4 software in 3D mode. Table 1 and 2 present the dimensions of 8 different proposed designs according to Figs. 3 and 4. The second column of the Table 2 delineates the geometry of the cantilever structure, distinguishing between triangular and rectangular configurations. The fourth column is dedicated to specifying the constituent materials of the lower and upper layers of the cantilever beam. Furthermore, the dimensions of the cantilever beam are provided in the fifth

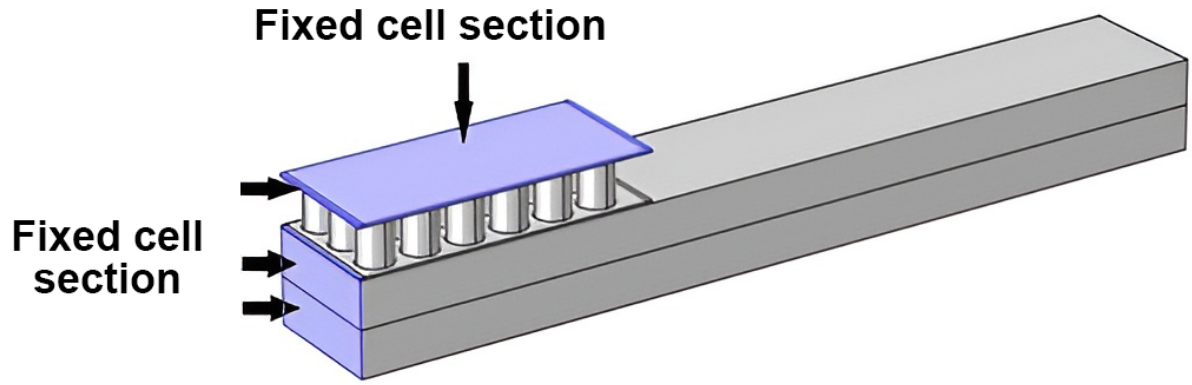

Figure 7. Proposed hybrid solar cell with the most considerable piezoelectric length.

column, while the sixth column details the dimensions of the piezoelectric separator. Finally, the last column quantifies the number of nanowires incorporated within the piezoelectric separator. Specifically, the upper layers of the cantilever beam are made of aluminum and copper, while the lower layer is made of SiO_2.

The nanowires are placed so that the rods are placed between two panels of the rods themselves, because they cannot be released freely. This panel also acts as a terminal for extracting the voltage and current of the solar cell. As shown in Fig. 8, the solar cell current is extracted using an electrical circuit consisting of a resistor and a 1 V DC source.

According to Fig. 9, since one side of the beams is fixed and the other side is free, due to the difference in coefficient of expansion and heat, the maximum stress will be created in the fixed part where the piezo part is located with the nanowires. Due to the maximum stress at the fixed end of the solar cells, the piezo section in the designs should be much shorter than the size of the beams. For this reason, the size of this section is much smaller and its length is selected according to Accordingly, the lengths of this section are selected as 10 µm and 20 µm, corresponding to 5% and 10% of the beam

Table 1. Design parameters of proposed MEMS solar cell.

Parameter	Recommended Value/Range	Unit
Electron Mobility	100-200	$cm^2/V{\cdot}s$
Hole Mobility	10-50	$cm^2/V{\cdot}s$
Nanowire Spacing (Pitch)	100-300	nm
Relative Permittivity (ε_r)	8.5-9.5	
Young's Modulus (E) ZnO	208 GPa	
Young's Modulus (E) AlN	340 GPa	
Young's Modulus (E) Cu	110 GPa	
Young's Modulus (E) Al	70 GPa	
Nanowire Spacing (Pitch)	10-30	nm
Absorption Coefficient	10^3-10^4	cm^{-1}
Piezoelectric Coefficient (d_{33}) ZnO	12.3	pC/N
Piezoelectric Coefficient (d_{33}) AlN	5.3	pC/N
Thermal Expansion Coefficient (α) ZnO	4.31×10^{-6} K^{-1}	
Thermal Expansion Coefficient (α) AlN	4.2×10^{-6} K^{-1}	
Thermal Expansion Coefficient (α) Al	$\approx 23.1 \times 10^{-6}$ K^{-1}	
Thermal Expansion Coefficient (α) Cu	$\approx 16.5 \times 10^{-6}$ K^{-1}	
Thermal Expansion Coefficient (α) SiO_2	0.5×10^{-6} K^{-1}	
Curie Temperature (T_c) ZnO	300	k
Curie Temperature (T_c) AlN	1150	°C

https://dx.doi.org/10.57647/mjee.2026.2001.07

Table 2. Dimensions and Design parameters of the projected MEMS solar cell.

Proposed design	Type	Layers	Material	Dimension* (µm)	Piezoelectric dimension	Nanowires pieces
1	rectangular	Lower layer	SiO_2	200×10×2	10×10×1	9
		upper layer	Al	200×10×2		
2		Lower layer	SiO_2	200×10×4	20×10×1	18
		upper layer	Cu	200×10×4	60×20×2	
3		Lower layer	SiO_2	200×10×2	10×10×1	9
		upper layer	Al	200×10×2		
4		Lower layer	SiO_2	200×10×4	20×10×1	18
		upper layer	Cu	200×10×4	60×20×2	
1	triangular	Lower layer	SiO_2	200×10×2	10×10×1	9
		upper layer	Al	200×10×2		
2		Lower layer	SiO_2	200×10×4	20×10×1	18
		upper layer	Cu	200×10×4	60×20×2	
3		Lower layer	SiO_2	200×10×2	10×10×1	9
		upper layer	Al	200×10×2		
4		Lower layer	SiO_2	200×10×4	20×10×1	18
		upper layer	Cu	200×10×4	60×20×2	

length, respectively (see Table 1). It should be noted that in this paper, the number of nanowires is considered to be different so that there are other output results. Figure 9 shows the proposed piezoelectric structure with 18 nanowires and fixed parts.

Figure 9 shows the proposed structure containing 18 nanowires arranged in six rows. Each has a diameter of 2 µm and a length of 1 µm. The layers holding the nanowires are thin and made of piezoelectric material (ZnO) with a thickness of 0.05 µm. According to the values of different layers The structure of the solar cell is subjected to a sinusoidal heat flux given by $1000 \times \sin(80t)$.

Figure 10 shows applying heat to the upper surface of the proposed piezoelectric structure.

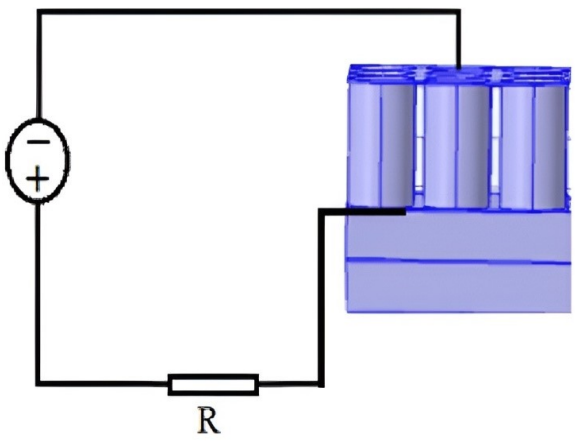

Figure 8. Electrical circuit to extract current from a solar cell.

The amount of stress distribution is shown in Fig. 11 and indicates that, this amount was higher at the fixed end of the cantilever (lighter color) and proves the claim that the piezoelectric should be in this position. The maximum stress value in the proposed structure is 4.5×10^6 N/m^2. Figure 12 shows the effect of stress on nanowires, which results in changes in nanowires and voltage.

According to Fig. 12, it is understood that the stress created did not cause the same and one-sided changes in the nanowires. The reason for this is that the end of the beam and the currents and fields between the nanowires are fixed which in the [27], this is much more than the proposed design in this study, and that is why the output current has not been extracted sinusoidally. In this research, an attempt has been made to improve the results of [27].

The results related to temperature changes in the structure are given in Fig. 13. In this figure, the temperature change compared to the initial temperature of the structure is presented. At the free end of the cantilever, there are many temperature changes. Since the bottom layer (SiO_2) has a lower CTE than the top layer (aluminum), the bilayer structure deflects along the z axis. When it reaches its maximum deviation, it returns to its original state as the temperature decreases. Also, the results related to temperature change over time presented in Fig. 14. Figure 14 shows the cantilever surface temperature at $t = 2$ s and $t = 10$ s. According to the figure, at early times, the surface temperature is higher. over time,

https://dx.doi.org/10.57647/mjee.2026.2001.07

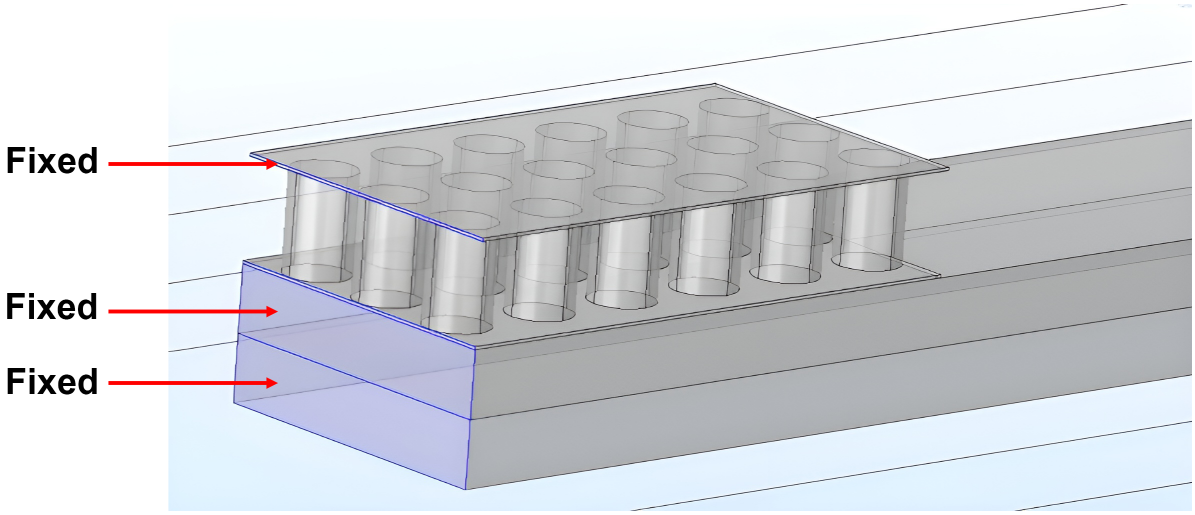

Figure 9. Fixed parts of the beam in the simulations with 18 nanowires in 6 rows.

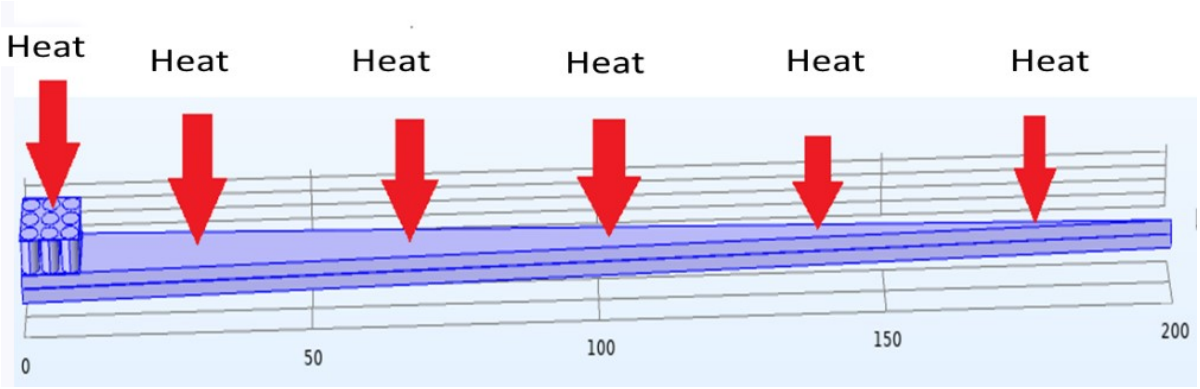

Figure 10. Applying heat to the upper surface of the proposed piezoelectric structure.

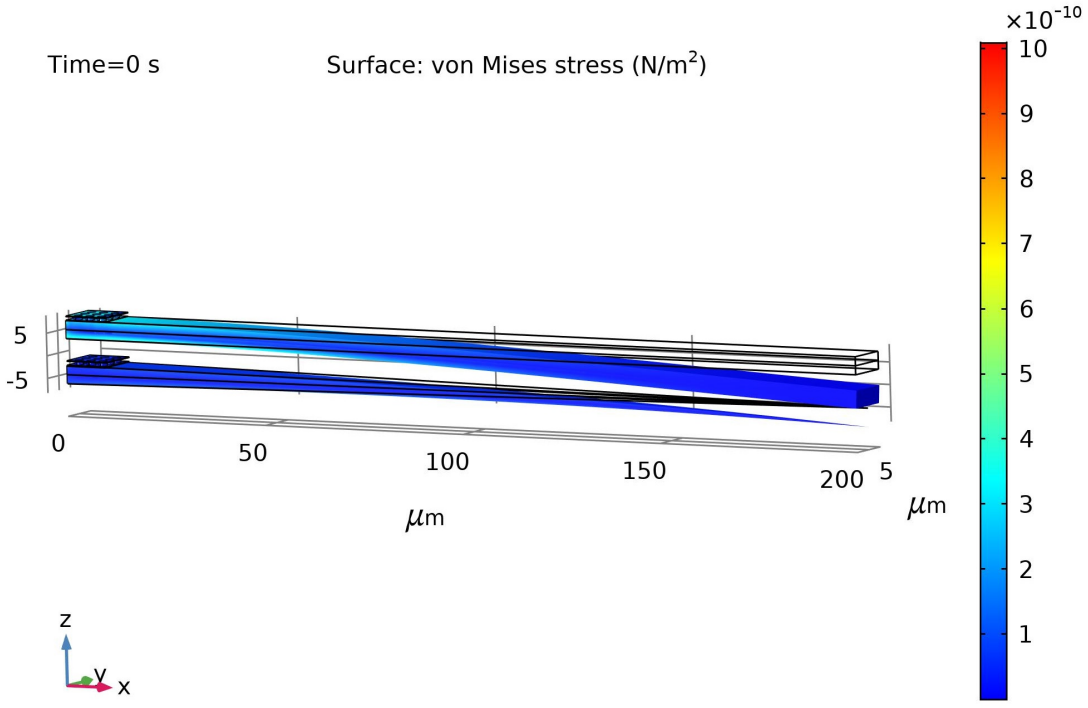

Figure 11. The amount of stress distribution in different layers.

https://dx.doi.org/10.57647/mjee.2026.2001.07

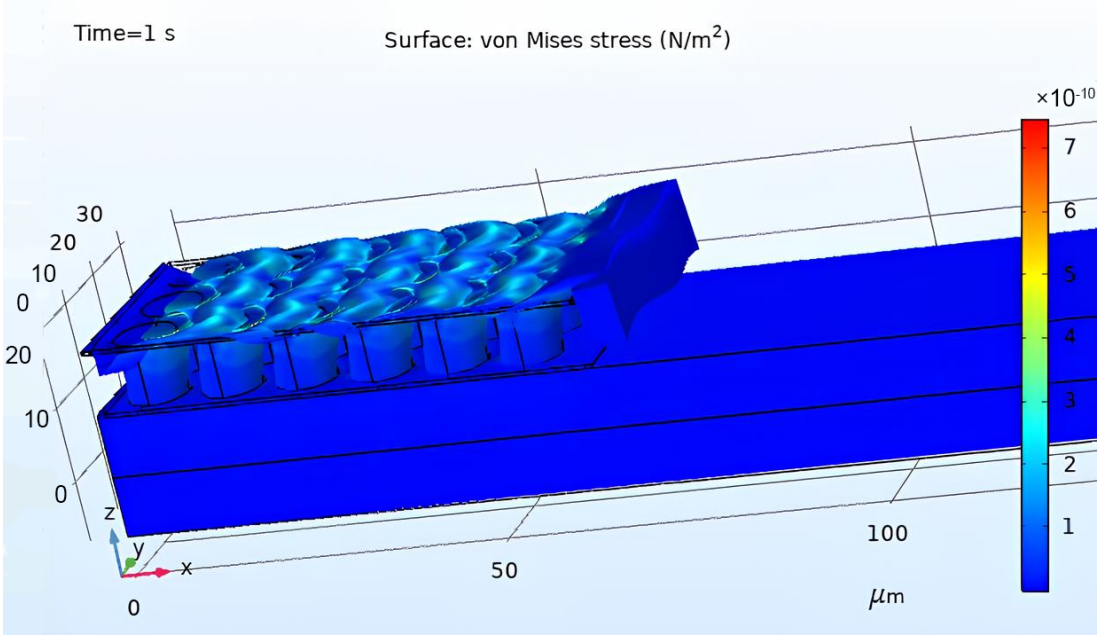

Figure 12. Impact of stress created at the fixed end of a structure with 18 nanowires.

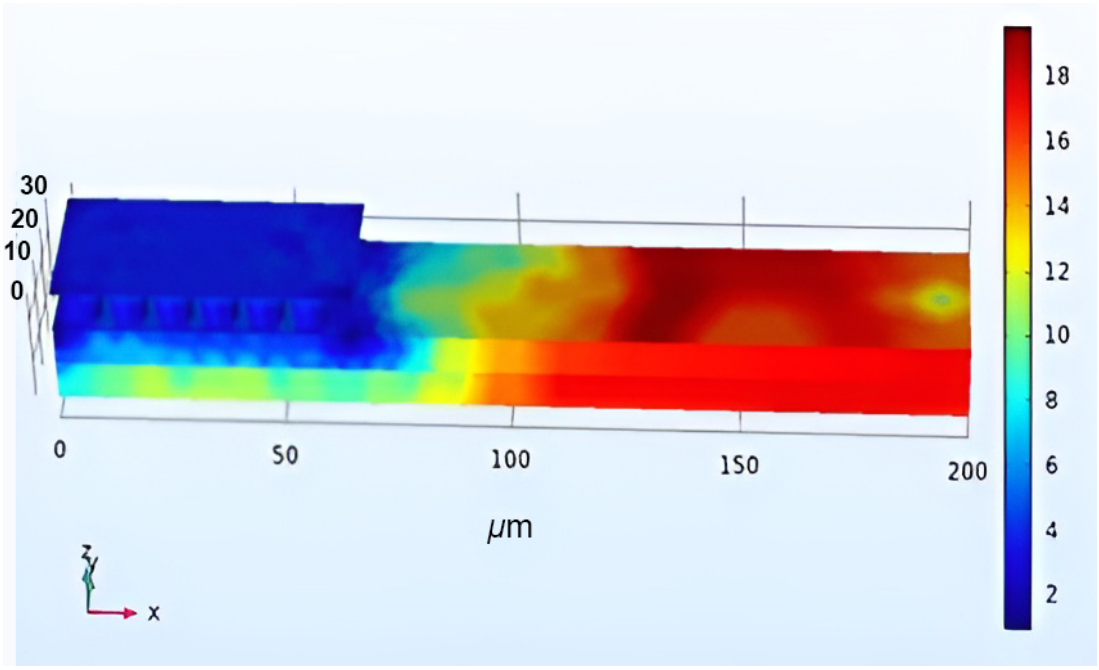

Figure 13. Temperature change in the proposed structure compared to the initial temperature.

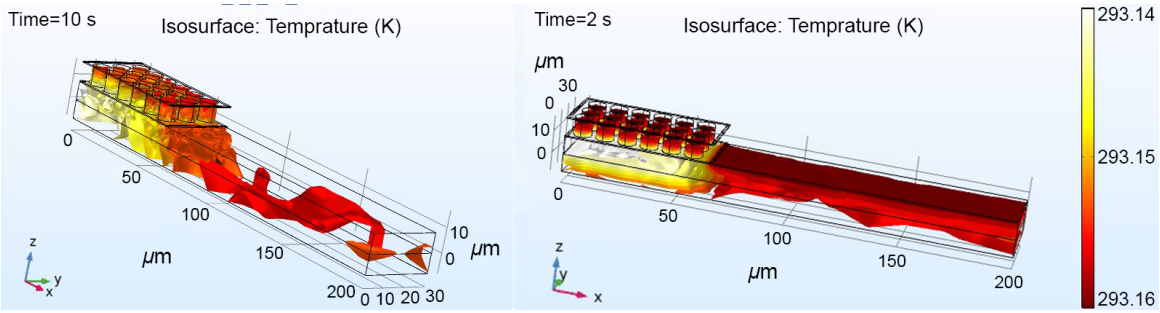

Figure 14. Temperature change during time in the proposed structure.

https://dx.doi.org/10.57647/mjee.2026.2001.07

this temperature became more balanced and because it is entered sinusoidally, it will change over time.

Figure 15 shows that the maximum displacement for the rectangular state is about 4 µm and for the triangular state is about 6 µm at the free end of the solar cell, which is due to the heat difference between the two materials (Si and Al) and the fixed part is prepared to generate electricity by piezoelectric effect.

To measure the voltage of the proposed design the structure is placed in series with a linear 1 kΩ resistor as shown in Fig. 8 and the voltage is measured on it, which is equal to the voltage of the proposed solar cell. The following are the results of the output voltage and current of structures with 9 and 18 nanowires with Al and SiO_2 substrates in Figs. 16 to 23.

Regarding Figs. 16 to 23, the essential results are expressed below:
a) The smaller the structure width and the number of nanowires, the better the current passes through the nanowires and the lower the loss rate compared to the case where the number of nanowires and the structure width are higher. These results are well seen in Figs. 16-19 that the generated voltage is very close to 1 volt and the net current between the nanowires also performs better.
b) In Figs. 20–23, with increasing area of the piezoelectric device and width of the structure, the net voltage slightly decreases compared to the previous configuration, while the net current through the nanowires remains acceptable.However, they have lower performance than the last mode.
c) Triangular structures generate a higher voltage than rectangular structures due to higher stress at the fixed ends of the beams.

4. Comparing efficiency with similar structures

Similar structures that have been designed and implemented in line with this paper, as well as the proposed design, use two different layers in addition to the piezoelectric material. The innovation presented in this paper is completely different from other similar designs. This innovation is the use of triangular structures and vertical nanowires in micro size (MEMS) as piezoelectric in the structure of the solar cell to reduce current and noise fields, which in the [26], this field and additional currents have caused an undesirable output current. There are several methods to obtain solar cell efficiency, one of which is to use (14):

$$\eta = \frac{P_{\text{out}}}{P_{\text{in}}} = \frac{V_m I_m}{P_{\text{in}}} = \frac{FF \times V_{oc} \times I_{sc}}{I_{\text{Illumination}} \times \text{Area}} \tag{14}$$

where FF is Fill factor, V_m and I_m are the voltage and current at the maximum output power of the solar, IIllumination is the amount of heat flux applied Area the surface area on which the heat flux enters is similar to [28]. Using (14), the efficiency of the MEMS solar cell (in different dimensions) can be obtained according to (14), the surface area on which the heat flux is applied is first calculated. This area equal to the total area seen from the top of the cell. Considering that the length of the cell is equal to 200 µm and its width is selected at 20 µm/10 µm, the total area will be 4000 μm^2/2000 μm^2. The amount of heat flux is applied is also 1000 W/m^2. The FF coefficient is also calculated using equation(15).

$$FF = \frac{V_m I_m}{V_{oc} \times I_{sc}} \tag{15}$$

The value of this parameter never reaches one but approaches unity. By substituting equation(15) into (14),

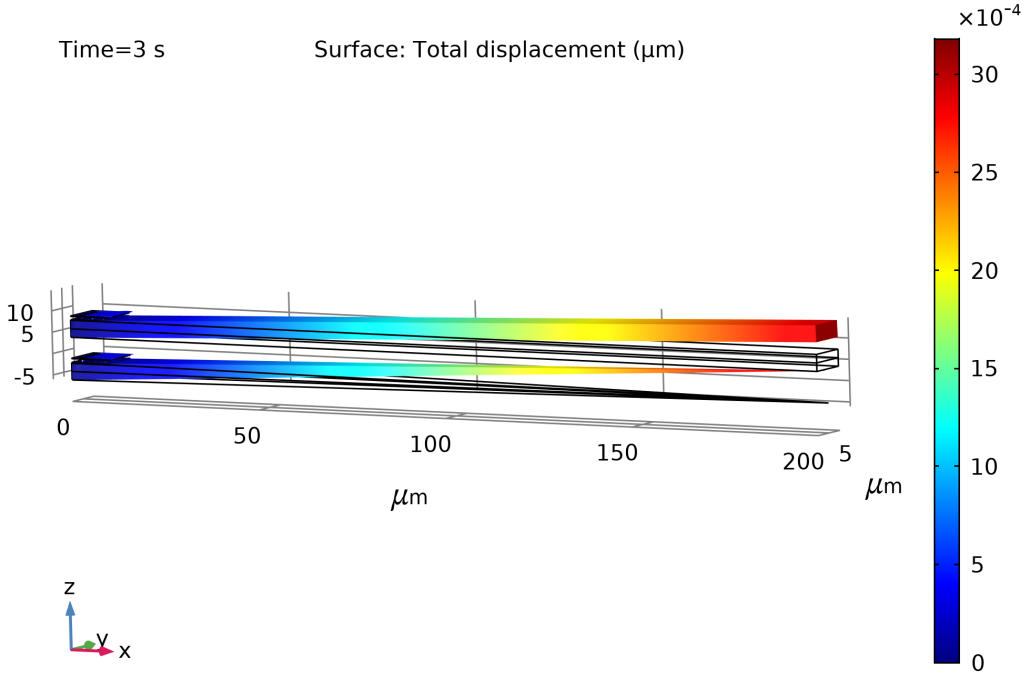

Figure 15. The amount of displacement of the free end of the cantilever.

https://dx.doi.org/10.57647/mjee.2026.2001.07

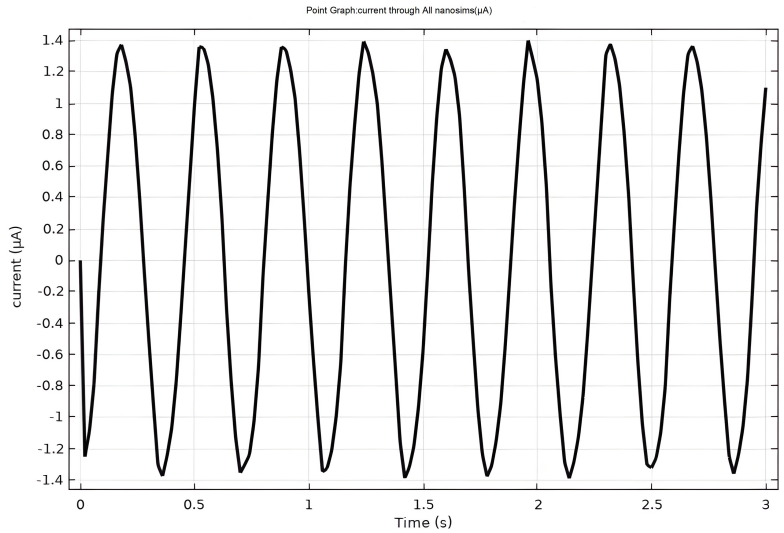

Figure 16. Current generated in a rectangular solar cell with 9 nanowires in 3 rows with a structure size of 200 × 10 × 2 µm.

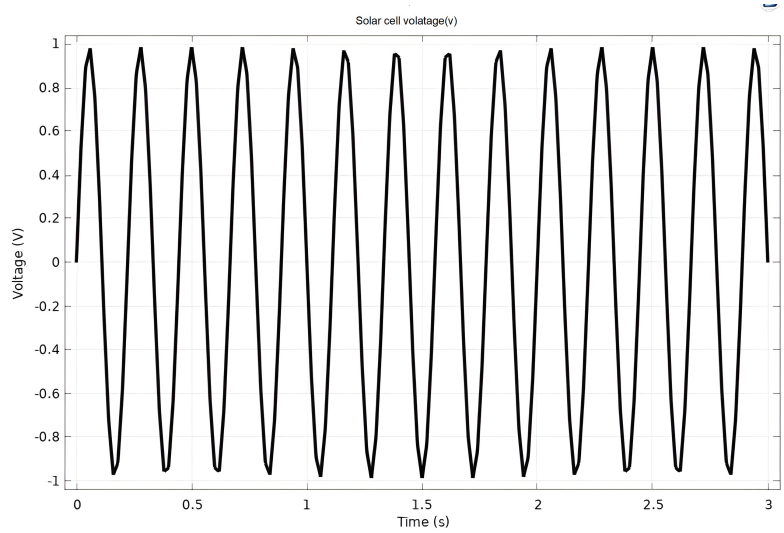

Figure 17. Voltage generated in a rectangular solar cell with 9 nanowires in 3 rows with a structure size of 200 × 10 × 2 µm.

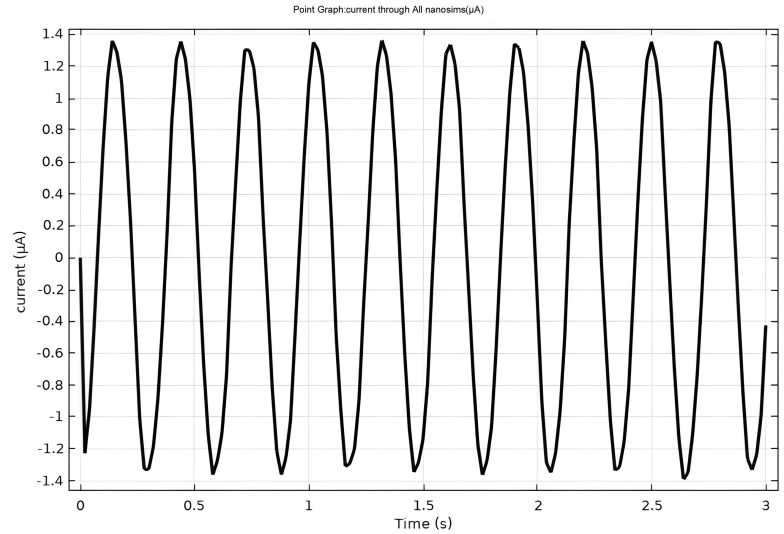

Figure 18. Current generated in a triangular solar cell with 9 nanowires in 3 rows with a structure size of 200 × 10 × 2 µm.

https://dx.doi.org/10.57647/mjee.2026.2001.07

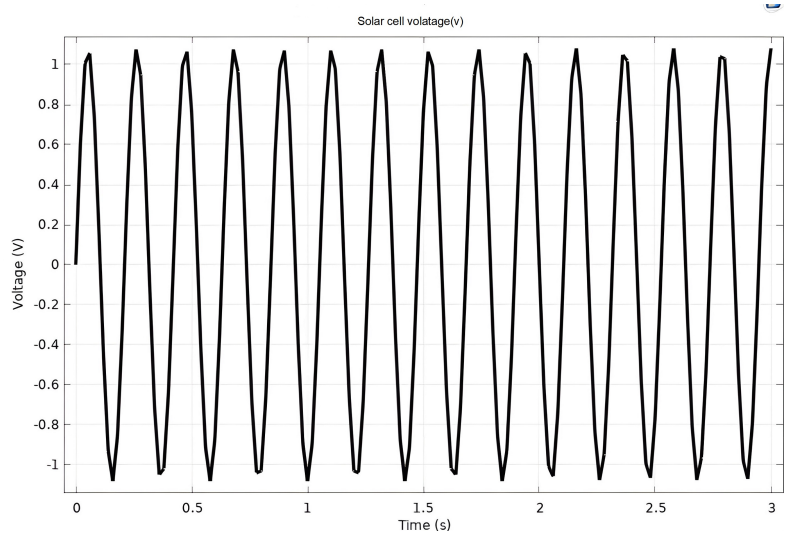

Figure 19. Voltage generated in a triangular solar cell with 9 nanowires in 3 rows with a structure size of 200 × 10 × 2 µm.

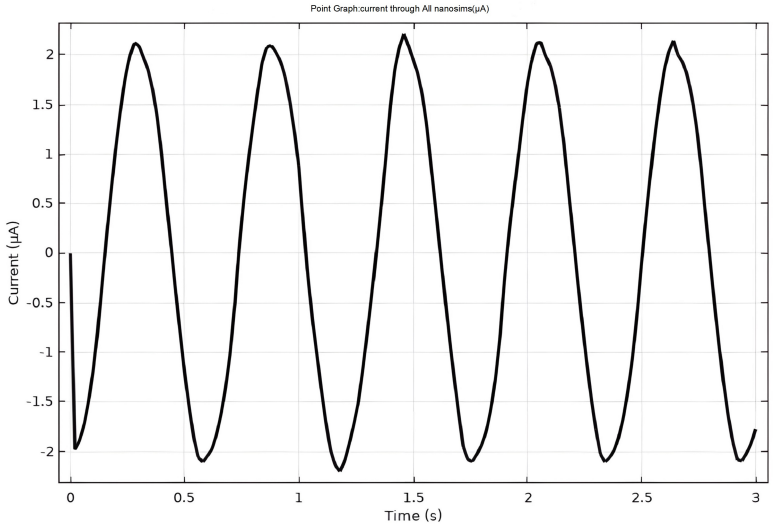

Figure 20. Current generated in a rectangular solar cell with 18 nanowires in 6 rows with a structure size of 200 × 20 × 2 µm.

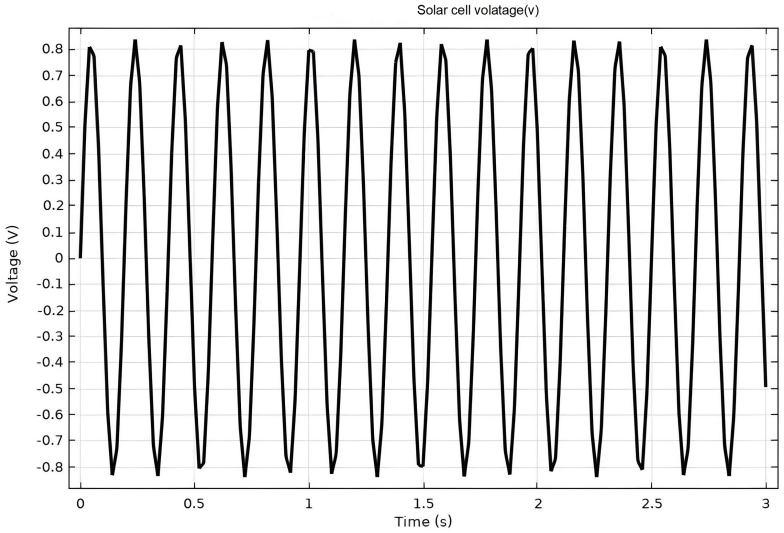

Figure 21. Voltage generated in a rectangular solar cell with 18 nanowires in 6 rows with a structure size of 200 × 20 × 2 µm.

https://dx.doi.org/10.57647/mjee.2026.2001.07

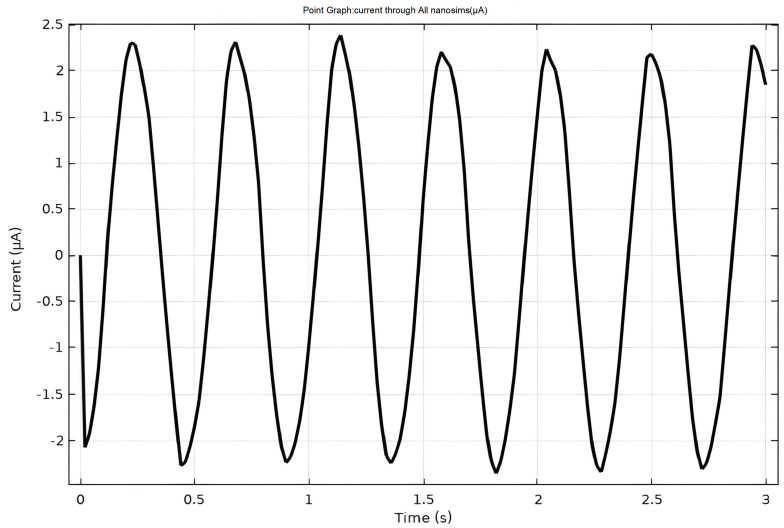

Figure 22. Current generated in a triangular solar cell with 18 nanowires in 6 rows with a structure size of 200 × 20 × 2 μm.

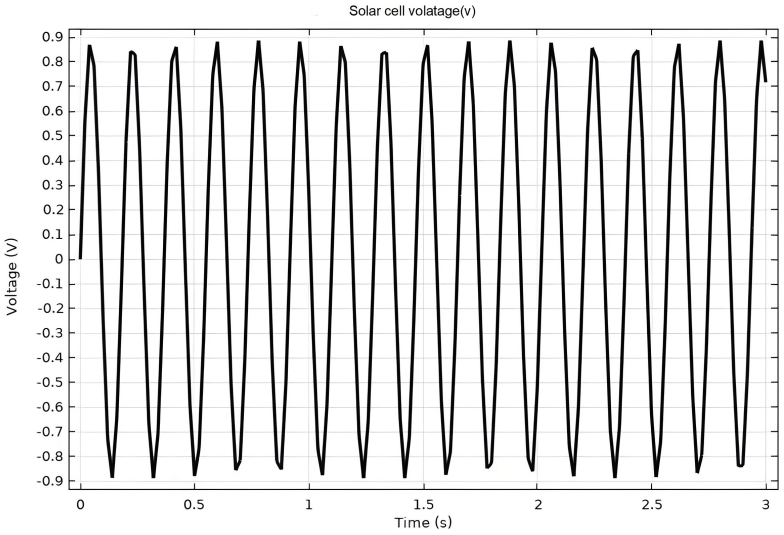

Figure 23. Voltage generated in a triangular solar cell with 18 nanowires in 6 rows with a structure size of 200 × 20 × 2 μm.

the efficiency is obtained as:

$$\eta = \frac{V_m I_m}{I_{\text{Illumination}} \times \text{Area}} \tag{16}$$

To calculate the efficiency of the proposed hybrid solar cell according to (13), at the voltage and current output of each structure the maximum value of voltage and current in the relevant diagram is calculated and placed in the equation. For example, in Fig. 19, the maximum current where each period sees its output (actually the minimum value of the peaks) is 2.23 μA, and the maximum voltage in this figure is equal to 0.86 V.

Table 3 presents the results of the efficiency and FF for each structure with Al as the upper layer material.

This paper aimed to design a solar cell with a MEMS structure that can receive more energy from solar radiation and also generate high electrical voltage. The MEMS solar cell structures presented in Table 4 have largely failed to provide the expected results of a solar cell.

Therefore, the proposed structure is compared with the results of photovoltaic solar cells. On the other hand, because in this paper we have only worked on the output voltage of the cell. Therefore, the proposed structure is compared only in terms of output voltage and surface area of the solar energy receiver.

According to Table 4, the proposed design has different operating rules compared to photovoltaic solar cells and .it is capable of generating almost the same voltage but the energy receiving surface of this structure is much smaller. Also, in this design we have been able to create a variable electrical voltage by using a certain number of nanowires made of piezoelectric material. This itself is an advantage because while the such a structure can be used directly without the need for a converter.

This study is a theoretical analysis and forms the basis for doing practical and detailed work in the future, and the results are obtained in a simulation environment without getting the consideration of some practical details.

Table 3. Efficiency and FF coefficient of different proposed structures.

Type	Nanowires pieces	Efficiency	FF
rectangular	9 pieces with a width of 10	42.45%	0.90
	9 pieces with a width of 20	43.72%	0.87
	18 pieces with a width of 10	43.9%	0.87
	18 pieces with a width of 10	41.34%	0.85
triangular	9 pieces with a width of 10	46.11%	0.91
	9 pieces with a width of 20	45.61%	0.90
	10 pieces with a width of 18	44.37%	0.87
	18 pieces with a width of 20	43.91%	0.88

Table 4. Comparison of the proposed design with previous researches.

Ref.	Open circuit voltage (V)	Area (mm^2)	Efficiency	FF
[18]	0.75	0.004	-	-
[27]	0.90	0.004	40%	-
[29]	0.63	6	-	-
[30]	0.94	0.004	24.2%	0.82
[31]	0.55	110	11.8%	0.75
Proposed design	1.15	0.004	46.11%	0.91

surely, considering the practical limitations of the real implementation, the efficiency will be lower, however, the results obtained from the simulation are promising. It shows an improvement in efficiency compared to previous similar works, although the degree of practical improvement is lower than the theoretical result obtained in the paper.

5. Conclusion

In this paper, the process of designing and simulating a MEMS solar cell is thoroughly analyzed. To implement the proposed structure, new solar cells, and piezoelectric devices have been implemented separately with the help of some of piezoelectric nanowires (PZT or (Lead Zirconate Titanate (PZT-5H)) with COMSOL software. Finally, the solar cell was fabricated using piezoelectric nanowires and two-layer beams made of silicon and aluminum. The bottom layer is made of silicon with a length of 200 µm, a width of 10 µm or 20 µm, and a thickness of 2 µm. The top layer is made of aluminum and similar to the bottom layer has a length of 200 µm, a width of 20 µm and a thickness of 2 µm. The piezoelectric structure consists of several nanowires that include 18 and 9 nanowires used in the simulation. After determining the dimensions and material of the layers, this structure was implemented in COMSOL software and the results related to stress, displacement and voltage of different parts of the structure were stated. After comparing with similar researches in Table 4, it was shown that the proposed structure has a better function compared to similar researches.

Authors contributions
All authors contributed equally to the conception, design, execution, and writing of this work. All authors read and approved the final manuscript.

Availability of data and materials
The authors declare that the data supporting the findings of this study are available within the paper.

Conflict of interests
The authors assert that they do not have any identifiable conflicting financial interests or personal relationships that might be perceived to influence the work presented in this paper.

References

1. Torkashvand Z, Shayeganfar F, and Ramazani A. "**Advances of materials science in MEMS applications: A review.**" Results in Engineering 2024; 22:102115. DOI: 10.1016/j.rineng.2024.102115
2. Lyshevski SE. "**MEMS and NEMS: Systems, Devices, and Structures**". 2002; CRC Press:3–18. DOI: 10.1201/9781315220246
3. Tayel MB and Ragab Y. "**A novel design of a MEMS solar cell based on microcantilever-photoinduced bending.**" International Conference on Innovative Engineering Systems, Alexandria, Egypt 2012 :41–45. DOI: 10.1109/ICIES.2012.6530842

4. Singh MM, Lim Y, and Manaf A. "**Smart Home using Microelectromechanical Systems (MEMS) sensor and ambient intelligences (SAHOMASI)**". Lecture Notes in Electrical Engineering 2018; 14:557–567. DOI: 10.1007/978-981-13-2622-6_54
5. Mishra M, Dubey V, Mishra PM, and Khan I. "**MEMS Technology: A Review.**" Journal of Engineering Research and Reports 2019; 4:1–24. DOI: 10.9734/jerr/2019/v4i116891
6. Sharma SK, Mishra RK, and Kumar A. "**A review on RF micro-electro-mechanical-systems (MEMS) switch for radio frequency applications.**" Microsystem Technologies 2021; 27:765–786. DOI: 10.1007/s00542-020-05025-y
7. Goodnick SM and Honsberg C. "**Solar cells. In: Handbook of Semiconductor Devices** ". 2022; Springer:699–745. DOI: 10.1007/978-3-030-79827-7_19
8. Vincent P, Shin SC, Goo J, You YJ, Cho B, Lee S, Lee DW, Kwon SR, Chung KB, Lee JJ, Bae JH, Shim JW, and Kim H. "**Indoor-type photovoltaics with organic solar cells through optimal design.**" Dyes and Pigments 2018; 159:306–313. DOI: 10.1016/j.dyepig.2018.06.025
9. Lu L, Yang Z, Meacham K, Cvetkovic C, Corbin EA, Vázquez-Guardado A, Xue M, Yin L, Boroumand J, Pakeltis G, Sang T, Yu KJ, Chanda D, Bashir R, Gereau RW, Sheng X, and Rogers JA. "**Biodegradable monocrystalline silicon photovoltaic microcells as power supplies for transient biomedical implants.**" Advanced Energy Materials 2018; 8. DOI: 10.1002/aenm.201703035
10. Sun H, Yin M, Wei W, Li J, Wang H, and Jin X. "**MEMS based energy harvesting for the Internet of Things: a survey.**" Microsystem Technologies 2018; 24:2853–2869. DOI: 10.1007/s00542-018-3763-z
11. Patel S, Scheideler WJ, Karim MA, and Subramanian V. "**Inkjet-printed MEM relays for active solar cell routing.** " IEEE Micro Electro Mechanical Systems (MEMS) Conf. 2018 :616–619. DOI: 10.1109/memsys.2018.8346629
12. Akbari A and Keshmiri SH. "**Efficiency Enhancement of a Tandem Perovskite-Silicon Solar Cell.**" Majlesi Journal of Electrical Engineering 2024; 18:1–7. DOI: 10.57647/j.mjee.2024.180349
13. Gai B, Geisz JF, Friedman DJ, Chen H, and Yoon J. "**Printed assemblies of microscale triple-junction inverted metamorphic GaInP/GaAs/InGaAs Solar Cells.**" Progress in Photovoltaics: Research and Applications 2019; 27:520–527. DOI: 10.1002/pip.3127
14. Kharel K and Freundlich A. "**III-V dilute nitride quantum-engineered solar cell for lattice-matched silicon-based tandems.**" Physics, Simulation, and Photonic Engineering of Photovoltaic Devices VIII 2019; 1:39–46. DOI: 10.1117/12.2510813
15. Green MA, Emery K, Hishikawa Y, Warta W, and Dunlop ED. "**Solar Cell Efficiency Tables (version 45)**". Progress in Photovoltaics: Research and Applications 2014; 23:1–9. DOI: 10.1002/pip.2573
16. Nielson GN, Okandan M, Cruz-Campa JL, Resnick PR, Sanchez CA, Sweatt WC, Lentine AL, Gupta VP, and Nelson JS. "**Next generation photovoltaic cells and systems through MEMS technology.**" ECS Transactions 2012; 44:1347–1352. DOI: 10.1149/1.3694470
17. Yunus NHM, Sampe J, Yunas J, and Pawi A. "**MEMS Based RF Energy Harvester for Battery-Less Remote Control: A Review.**" American Journal of Applied Sciences 2017; 14:316–324. DOI: 10.3844/ajassp.2017.316.324
18. Mehdizadeh SN and Ganji BA. "**Design and simulation of small size MEMS bimaterial cantilever solar cell using piezoelectric layer.**" Microsystem Technologies 2017; 23:5849–5854. DOI: 10.1007/s00542-017-3491-9
19. Kim K, Hwang MB, Jeong J, Min NK, and Kwon KH. "**Micromachining of a bimorph Pb(Zr,Ti)O_3(PZT) cantilever using MEMS process for energy harvesting application.**" Journal of Nanoscience and Nanotechnology 2012; 12:6011–6015. DOI: 10.1166/jnn.2012.6365
20. Baughman DC. "**Creation and optimization of novel solar cell power via bimaterial Piezoelectric MEMS device.**" 2011; Ph.D. dissertation, Naval Postgraduate School, Monterey, California
21. Zhu M, Worthington E, and Njuguna J. "**Coupled piezoelectric-circuit FEA to study influence of a resistive load on power output of piezoelectric energy devices.** " Smart sensors, Actuators and MEMS IV 2009 :17–28. DOI: 10.1117/12.822829
22. Dang C, Zhang S, Li X, Wang Y, and Liu H. "**System integration for solar-driven interfacial desalination.**" Device 2024; 2:1–20. DOI: 10.1016/j.device.2024.100361
23. Beer FP, Jr. ERJ, DeWolf JT, Mazurek DF, Anderson PM, Hirth JP, and Lothe J. "**Mechanics of Materials, 7th ed.**" 2017; New York: McGraw-Hill:430–50. DOI: 10.1036/9781260463510
24. Xu Q, Gao A, Li Y, and Jin Y. "**Design and optimization of piezoelectric cantilever beam vibration energy harvester.** " Micromachines 2022; 13:675. DOI: 10.3390/mi13050675

25. Voicu RC, Tibeica C, Müller R, Dinescu A, Pustan M, and Birleanu C. "**Design, simulation and testing of polymeric microgrippers with V-shaped electrothermal actuators and encapsulated heaters.**" International Semiconductor Conference (CAS), Sinaia, Romania 2016 :89-92. DOI: 10.1109/SMICND.2016.7783048

26. Qiao S, Liu J, Fu G, Ren K, Li Z, Wang S, and Pan C. "**ZnO nanowire based CIGS solar cell and its efficiency enhancement by the piezo-phototronic effect.**" Nano Energy 2018; 49:508–514. DOI: 10.1016/j.nanoen.2018.04.070

27. Ganji BA and Teymurnejad R. "**Efficiency improving of NEMS solar cell using piezoelectric nanowires.**" Microsystem Technologies 2020; 27:649–657. DOI: 10.1007/s00542-020-04967-7

28. Mishra VL, Chauhan YK, and Verma KS. "**Various Modeling Approaches of Photovoltaic Module: A Comparative Analysis.**" Majlesi Journal of Electrical Engineering 2023; 17:117–131. DOI: 10.30468/mjee.2023.1984023

29. Köppel G, Amkreutz D, Sonntag P, Yang G, Swaaij RV, Isabella O, Zeman M, Rech B, and Becker C. "**Periodic and random substrate textures for liquid-phase crystallized silicon thin-film solar cells.**" IEEE Journal of Photovoltaics 2017; 7:85–90. DOI: 10.1109/JPHOTOV.2016.2618605

30. Wanleass M. "**Systems and methods for advanced ultra-high-performance InP solar cells.** " 2017; U.S. Patent:131

31. Sai H, Maejima K, Matsui T, Koida T, Matsubara K, Kondo M, Takeuchi Y, Sugiyama S, Katayama H, and Yoshida I. "**Effect of front TCO layer on properties of substrate-type thin-film microcrystalline silicon solar cells.**" IEEE Journal of Photovoltaics 2015; 5:1528–1533. DOI: 10.1109/JPHOTOV.2015.2478030